Cleaner Engineering and Technology 1 (2020) 100024

Contents lists available at ScienceDirect

Cleaner Engineering and Technology

journal homepage: www.journals.elsevier.com/cleaner-engineering-and-technology

Thermal performance of heat and water recovery systems: Role of condensing heat exchanger material

Negar Mohammadaliha, Mohammad Amani, Majid Bahrami *

Laboratory for Alternative Energy Conversion (LAEC), School of Mechatronic Systems Engineering, Simon Fraser University, BC, V3T 0A3, Canada

ARTICLE INFO

Keywords:
Heat and water recovery
Wet flue gas
Heat exchanger design
Thermal conductivity
Latent heat

ABSTRACT

A significant amount of sensible and latent heat can be recovered at low temperatures from the flue gas of process heating equipment. However, the condensation of acids and water vapor makes the flue gas a highly-corrosive environment, which is a challenge for condensing heat exchangers. Corrosion-resistant materials are usually expensive and/or have relatively low thermal conductivities. Hence, it is essential to characterize the role of thermal conductivity of heat exchanger material in the performance of condensing heat exchangers. In the present study, a new analytical model is proposed and validated against available experimental data to predict the thermal performance of a tube-bank heat and water recovery unit. Our study indicates a threshold for tube thermal conductivity (~0.75 W $m^{-1}K^{-1}$), which is a point where further increase does not significantly improve the condensation efficiency. This relatively low value of thermal conductivity, compared to commonly-used materials, e.g., ~10–15 W $m^{-1}K^{-1}$ for stainless steel, unlocks the potential of using materials such as natural graphite, plastics, polymers, and ceramics (with thermally conductive additives) for applications in condensing heat exchangers and heat/water recovery in industry.

1. Introduction

In the last few decades, there has been immense concern about the harmful environmental impacts of non-renewable energy systems, including climate change, environmental impacts, air pollution, as well as fears of facing a shortage of energy (Martins et al., 2018). Therefore, improving the cost and efficiency of renewable energy systems to replace fossil fuels have received immense attention (Ogbonnaya et al., 2019). A significant portion of energy used in industrial processes is released to the environment as waste heat (with temperatures below 100 °C). The recovery and reuse of industrial waste heat are beneficial and can reduce fossil fuel consumption, greenhouse gas emissions, and enhance efficiency by cutting the amount of heat loss (Men et al., 2019). The flue gas generated from the combustion of fossil fuels or biofuels in equipment, such as boilers, furnaces, and ovens is one of the primary sources of low-grade waste heat (Ammar et al., 2012). Waste heat recovery is more beneficial when temperatures are in the low-temperature range, as most industrial waste heat is in this category, as shown in Fig. 1.

The presence of water vapor in the flue gas of process heating equipment makes it possible to recover a considerable amount of latent heat at relatively low temperatures, along with the sensible heat of flue gas. The volume concentration of water vapor in the flue gas depends on the type of fuel burned in process heating equipment (Levy et al., 2008). Since natural gas has a higher hydrogen and lower carbon content compared to coal and oil, the flue gas of natural gas-fired combustion contains a higher concentration of water vapor. It also contains around 40% less CO_2 emission compared to coal; thereby, it is a promising candidate for waste water and latent heat recovery (de Gouw et al., 2014). Jeong et al. (2010) developed a model to estimate the condensation rate of water vapor in the flue gas and heat transferred from flue gas to cooling water and found that their results agree well with the experimental data. Xiong et al. (2017) studied the performance of a tube-bank heat exchanger made of fluorine plastic with an in-line arrangement of tubes for heat and water recovery from flue gas. They reported that 80% of the recovered heat came from recovering the latent heat while the share of sensible heat was only 20%, which clearly showed the significance of latent heat recovery. In a case study, Xiong et al. (2014) showed that 61.6 t/h of water could be potentially recovered using a heat and water recovery system in a 600 MW lignite-burned power plant, which was enough to run the desulfurization unit with zero-net water consumption. Hwang et al. (2010) evaluated a tube-bank heat exchanger with staggered and in-line crushed titanium tubes. After one year, they observed no sign of corrosion. That made titanium an

* Corresponding author.
E-mail address: mbahrami@sfu.ca (M. Bahrami).

https://doi.org/10.1016/j.clet.2020.100024
Received 22 September 2020; Received in revised form 28 November 2020; Accepted 29 November 2020

Nomenclature

A	area (m^2)
C_p	specific heat ($J.kg^{-1}.K^{-1}$)
d	dimeter (m)
f	Friction factor (−)
HEX	heat exchanger
h	convective heat transfer coefficient ($Wm^{-2}.K^{-1}$)
h_{fg}	latent heat of vaporization ($J.kg^{-1}$)
k	thermal conductivity ($W.m^{-1}.K^{-1}$)
k_m	convective mass transfer coefficient ($m.s^{-1}$)
Le	Lewis number of water vapor in flue gas (−)
M	molecular mass (kg)
$\dot{m}$	mass flow rate ($kg.s^{-1}$)
Nu	Nusselt number (−)
Pr	Prandtl number (−)
$\dot{Q}$	heat transfer rate (W)
R	thermal resistance ($K.W^{-1}$)
Re	Reynolds number (−)
S	tube pitch (m)
T	temperature (°C)
y	mole fraction of water vapor (−)

Greek letters

Δx	length of a unit cell (m)
ω	Humidity ratio (−)

Subscripts

c	cooling water
$cond$	condensation
g	flue gas
i	inner surface
in	inlet
int	interface
L	longitudinal direction
o	outer surface
out	outlet
s	tube surface
T	transverse direction
t	total

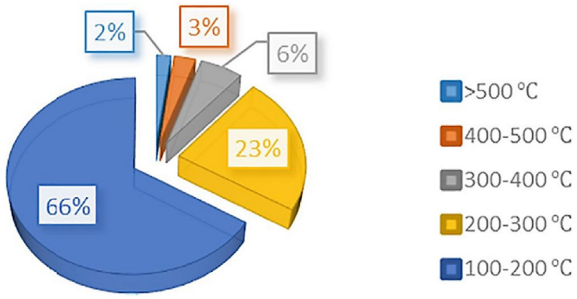

Fig. 1. Waste heat temperature distribution in industry (Haddad et al., 2014).

option for the corrosive environment. Moreover, the staggered arrangement of tubes resulted in a 50% higher Nusselt number compared to their in-line arrangement. Jia et al. (2001) investigated the performance of a spiral plate heat exchanger made of polytetrafluoroethylene (PTFE) for heat recovery from wet flue gas. Their results revealed that the heat transfer coefficient increases two-fold when compared with only sensible heat recovery from flue gas at the same temperature. Moreover, they concluded that using water and latent heat recovery systems is beneficial in decreasing the release of acidic and toxic chemicals into the ambient, which helps prevent acid rain. Shi et al. (2011) proposed a correlation for the Nusselt number of a compact fin-and-tube heat exchanger made of stainless steel with a staggered tube arrangement for heat recovery from humid air. They reported that both the friction factor and the Colburn factor for humid air increase with water vapor concentration. Li et al. (2016) introduced a new flue gas deep cooling method utilizing a flue gas desulfurization scrubber. Their system could recover latent heat and clean water at the same time. Han et al. (2017) also showed that the water recovery efficiency of a direct heat exchanger like a spray tower is higher than that of an indirect heat exchanger unit. Men et al. (2019) proposed a heat recovery system equipped with an enthalpy wheel. It was concluded that the dew point temperature of the discharged flue gas was greater than that of conventional flue gas, thereby recovering more latent heat.

Flue gas generated from the combustion of fossil fuels or biofuels may contain sulfur oxides (SO_x), nitrogen oxides (NO_x), hydrogen fluoride (HF), and hydrogen chloride (HCl) depending on the fuel's chemical composition (Zevenhoven and Kilpinen, 2001). Levy et al. (2008) showed that sulfuric acid (H_2SO_4), hydrochloric acid (HCl), and nitric acid (HNO_3) were condensed along with water vapor in the heat and water recovery unit due to the same range of dew point temperature of these acidic vapors and water vapor. They also reported that the mercury concentration of the flue gas at coal-fired power plants decreased by 60% by passing through the condensing heat recovery unit. However, condensation of acids leads to corrosion in heat recovery equipment because of the formation of sulfuric acid and other corrosive chemicals. Therefore, condensing heat exchangers should be made of highly corrosion-resistant materials. Levy et al. (2011) carried out corrosion examinations on a wide range of materials, including steels, stainless steels, nickel alloys, aluminum, polymers, and graphite, under various temperatures and sulfuric acid concentrations. Their results revealed that Nickel alloys 22 and 690, and polymers, such as fluorinated ethylene propylene (FEP) and PTFE were suitable for a corrosive environment, even with a high concentration sulfuric acid.

Apart from corrosion resistance, more influential parameters consisting of thermal properties, fouling, weight, fabrication methods, and cost must be reflected in material selection for heat exchangers recovering latent heat from flue gas. Although, plastics and polymers can be used for such applications because of their lightweight, low cost, and good corrosion resistance properties, their thermal conductivities are relatively low. To the best of the authors' knowledge, there are no publications in the open literature investigating the role of the thermal conductivity of the material used for latent heat recovery from flue gas. Thus, the present study aims to assess the significance of thermal conductivity on condensing heat exchangers' overall efficiency. A new analytical model is developed that can accurately predict the performance of condensing tube-bank heat exchangers with any tube pattern. The comparison with experimental data shows reasonable accuracy for the proposed analytical model. Compared to numerical methods, the present model is significantly faster and includes all pertinent thermophysical properties and operational parameters.

2. Model development

An analytical model is proposed to investigate the thermal performance of a tube-bank heat exchanger composed of an in-line array of circular tubes. The tube-bank heat exchanger is considered to be a group of geometrical unit cells in the form of short straight tube segments. A thermal resistance network of the unit cells is proposed and shown in Fig. 2. This unit-cell approach - in the form of a tube segment with a

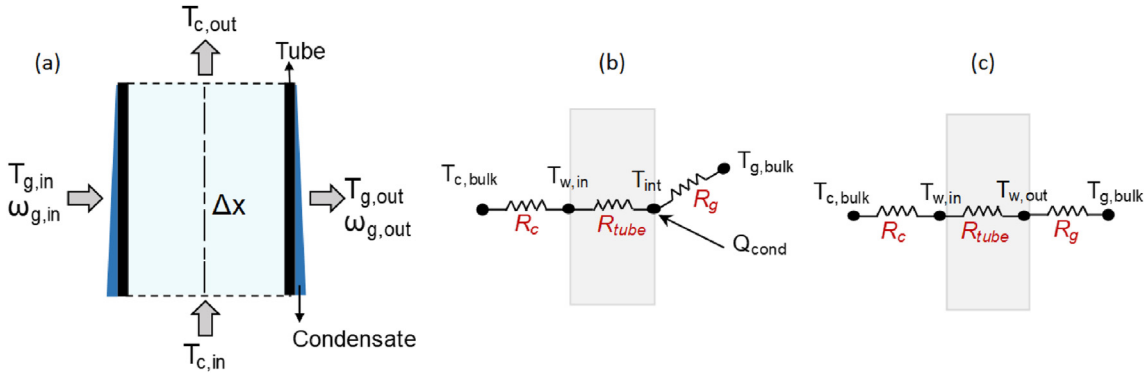

Fig. 2. a) Condensation of wet flue gas on a tube segment with a length of Δx; b) Thermal resistance network in the presence of condensation; and c) Thermal resistance network in the absence of condensation.

length of Δx is shown schematically in Fig. 2(a) - has been successfully adopted by Navarro and Cabezas-Gomez to model the performance of single-phase air-to-liquid cross-flow heat exchangers (Navarro and Cabezas-Gómez, 2005). Our developed model expands this approach to condensing heat exchangers in the presence of non-condensable gasses. The governing equations are solved for the unit cell, where the cooling water and flue gas flow inside and outside of the tubes, respectively. Based on the heat exchanger geometry, the tube segment can be placed vertically or horizontally in the flue gas flow. However, in both cases, the unit cell is a cross-flow heat exchanger. It is assumed that the cooling water is single-phase. When the tube surface temperature decreases below the dew point temperature of the flue gas, the water vapor in the flue gas starts to condense on the tube surface. In this case, as shown in Fig. 2(b), both sensible and latent heat is transferred to the cooling water through the heat exchanger wall. However, when the interface temperature is higher than the dew point temperature of the flue gas, only the sensible heat transfer occurs between the flue gas and cooling water. In this case, the thermal resistance network is simplified and shown in Fig. 2(c).

In the thermal resistance networks, see Fig. 2(b) and (c), the convective thermal resistance of cooling water and flue gas, are denoted by R_c and R_g, respectively, and defined as:

$$R_c = 1/(h_c A_{in}) \tag{1}$$

$$R_g = 1/(h_g A_{out}) \tag{2}$$

where, h_c and h_g are the convective heat transfer coefficients of cooling water and flue gas flows, and are calculated based on the correlation provided by Gnielinski (1976) (Eq. (3)) and Žukauskas (1972) (Eq. (4)), respectively.

$$Nu_{d,c} = \frac{h_c d}{k} = \frac{(f/8)(Re_d - 1000)Pr}{1 + 12.7(f/8)^{1/2}(Pr^{2/3} - 1)} \begin{cases} 3000 \le Re_d \le 5 \times 10^6 \\ 0.5 < Pr < 2000 \end{cases} \tag{3}$$

$$Nu_{d,g} = \frac{h_g d}{k} = C Re_{d,max}^{m} Pr^{0.36} (Pr/Pr_s)^{1/4} \; [0.7 < Pr < 500] \tag{4}$$

where, f is the friction factor; f for the smooth tubes can be calculated as:

$$f = (0.79 Ln(Re_d) - 1.64)^{-2} \tag{5}$$

It should be mentioned that the Reynolds number for Eq. (4) is calculated based on the tube diameter and maximum velocity of the flue gas flowing through the tubes. For the in-line tube arrangement and a $Re_{d,max}$ in the range of 10^3–2×10^5, the constants of C and m in Eq. (4) are equal to 0.27 and 0.63, respectively. However, at low Reynolds numbers ($100 \le Re_{d,max} \le 1,000$), the convective heat transfer coefficient of the gas flowing through a tube bank is the same as a single tube. In this case, the constants of C and m in Eq. (4) are equal to 0.51 and 0.5, respectively (Bergman et al., 2011). Moreover, the conductive thermal resistance of the tube's wall denoted by R_{tube} is defined as follows:

$$R_{tube} = Ln(d_o / d_i)/2\pi k \Delta x \tag{6}$$

where, k is the thermal conductivity of tube's material and d_i and d_o represent the inner and outer tube diameters, respectively. Zhang et al. (2018) showed that the effect of the thermal resistance of the liquid condensate layer is negligible, when the mass fraction of water vapor is less than 70%. Thus, the thermal resistance of the condensate layer is neglected in the present model, and the temperature of the outer tube surface is considered as the interface temperature, denoted by T_{int}, which is the temperature of the interface between the flue gas and the condensate layer.

In the absence of condensation, the energy balance is expressed according to the thermal resistance network as follows:

$$\left(T_{g,bulk} - T_{w,out}\right) / R_g = \left(T_{w,out} - T_{c,bulk}\right) / \left(R_{tube} + R_c\right) \tag{7}$$

However, in the presence of condensation, the unit cell energy balance is expressed as follows:

$$\dot{Q}_{cond} + \left(T_{g,bulk} - T_{int}\right) \Big/ R_g = \left(T_{int} - T_{c,bulk}\right) \Big/ \left(R_{tube} + R_c\right) \tag{8}$$

where, the condensation heat transfer, denoted by $\dot{Q}_{cond}$, is calculated by:

$$\dot{Q}_{cond} = k_m A_{out} h_{fg} \left(y_{bulk,g} - y_{int}\right) \tag{9}$$

where, k_m is the convective mass transfer coefficient, h_{fg} is the latent heat of vaporization of water vapor and $y_{bulk,g}$ and y_{int} are the mole fraction of water vapor in the bulk of gas and on the interface, respectively. $y_{bulk,g}$ is calculated based on the inlet humidity ratio of the flue gas as follows:

$$y_{bulk,g} = M_g \omega_g / M_{H_2O} \left(\omega_g + 1\right) \tag{10}$$

where, M_{H_2O} and M_g are the molecular mass of water vapor and flue gas, respectively. Moreover, y_{int} is calculated using Antoine's equation (Thomson, 1946). This equation is a class of semi-empirical correlations describing the relation between vapor pressure and temperature for pure substances. The Antoine equation is derived from the Clausius–Clapeyron relation.

Based on heat and mass transfer analogy (Lewis analogy) and equality of the Colburn j factors for heat and mass transfer, k_m is obtained from the following:

$$k_m = \left(h_g M_{H_2O}\right) / \left(c_{p,g} M_g y_{\ell m} Le^{2/3}\right) \tag{11}$$

where, $c_{p,g}$ is the specific heat of flue gas, and Le is Lewis number of water

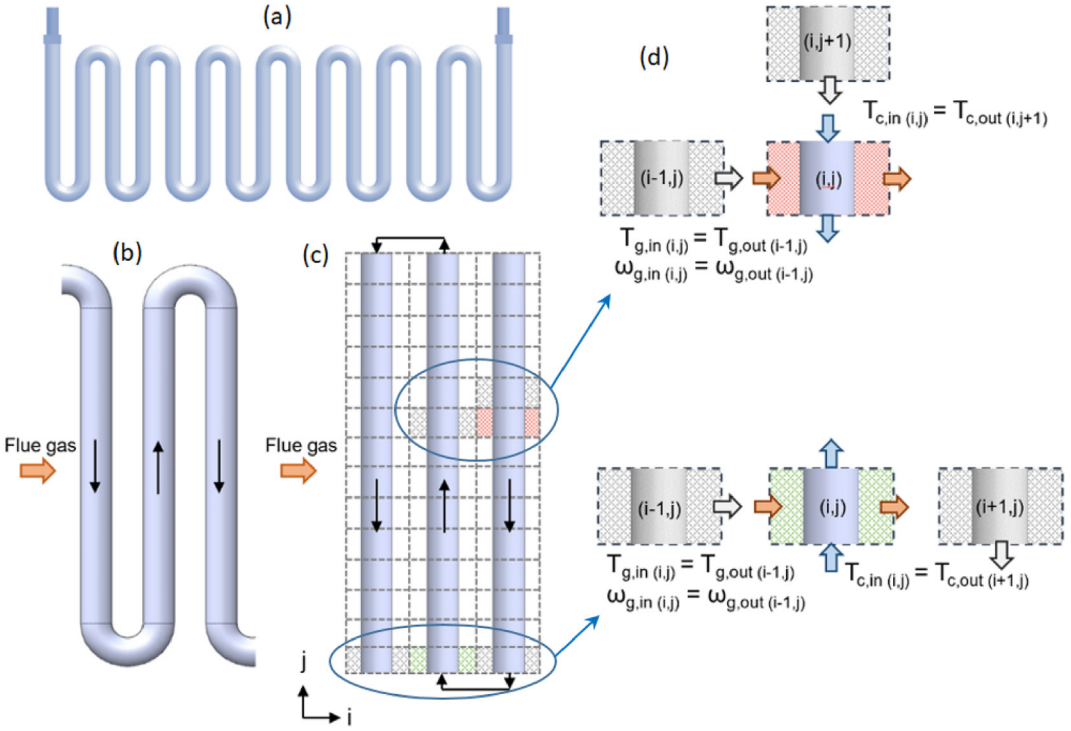

Fig. 3. a) A typical tube-bank heat exchanger with in-line tube arrangement; b) A portion of the tube-bank heat exchanger; c) computational domain; and d) The inlet conditions of two types of unit cells.

vapor in flue gas. Moreover, $y_{\ell m}$ is defined as:

$$y_{\ell m} = (y_{ni} - y_{nb}) / Ln(y_{ni} / y_{nb}) \tag{12}$$

where, y_{ni} and y_{nb} are the mole fraction of non-condensable gases at the interface and in the bulk of flue gas.

In the absence of condensation, solving the energy balance results in finding the tube's outer surface temperature, denoted by $T_{w,out}$; thus, the amount of sensible heat transferred from the flue gas to the cooling water can be calculated using Eq. (13). The sensible heat transfer leads to a decrease in the flue gas temperature and an increase in the cooling water temperature. In this case, the outlet temperature of the cooling water and flue gas are calculated using Eqs. (14) and (15).

$$Q_{non-cond} = h_g A_{out} \left(T_{g,bulk} - T_{w,out}\right) \tag{13}$$

$$T_{g,out} = T_{g,in} - \left(Q_{non-cond} \Big/ \dot{m}_g c_{p,g}\right) \tag{14}$$

$$T_{c,out} = T_{c,in} + \left(Q_{non-cond} \Big/ \dot{m}_c c_{p,c}\right) \tag{15}$$

In the presence of condensation, the interface temperature is calculated by solving the energy balance (Eq. (8)). In this case, sensible heat transferred from the flue gas to the cooling water leads to a decrease in the flue gas temperature. Moreover, the latent heat transferred to the cooling water dictates the condensation rate. Also, the total heat, including both latent and sensible, transferred to the cooling water causes an increase in the cooling water temperature. Therefore, in the presence of condensation, the outlet temperature of cooling water and flue gas along with the condensation rate are calculated using Eq. 16–18.

$$T_{g,out} = T_{g,in} - \left(\left(h_g A_{out}\ \left(T_{g,bulk} - T_{int}\right)\right) \Big/ \dot{m}_g c_{p,g}\right) \tag{16}$$

$$T_{c,out} = T_{c,in} + \left(T_{int} - T_{c,bulk}\right) \Big/ \dot{m}_c c_{p,c} (R_{tube} + R_c) \tag{17}$$

$$\dot{m}_{cond} = \dot{Q}_{cond} \Big/ h_{fg} \tag{18}$$

2.1. Unit cell approach

Fig. 3 schematically demonstrates how a tube-bank heat exchanger is modeled using the proposed unit cell approach. The model considers a tube bank as a parallel-tube group with identical diameter, spacing, and total length. The geometrical unit cells are in the form of tube segments, whose lengths depend on the number of unit cells along the tubes. Moreover, the number of unit cells along the flue gas direction depends on the number of tubes. It should be noted that the unit cells have the same geometry but different inlet conditions. Based on the unit cell's location, its inlet conditions are specified based on its adjacent unit cells or inlet conditions of the heat exchanger. Two main types of unit cells can be categorized in this modeling approach: i) unit cells placed along the tubes, an example is highlighted in red orange; and ii) unit cells placed at the top and bottom end of tubes, an example is highlighted in green. The only difference between these two unit cells is how their inlet conditions are specified. As shown in Fig. 3(c), the flue gas inlet conditions of both types of unit cells are specified based on the outlet conditions of their adjacent cells upstream. Furthermore, for unit cells in the middle, the inlet coolant temperature is considered equal to the outlet coolant temperature of its adjacent upstream cell in the coolant flow direction. However, for unit cells placed at the top and bottom ends, the inlet coolant temperature is considered equal to the outlet coolant temperature of the previous tube along the coolant flow direction.

2.2. Solution procedure and modeling results verification

The model solves the energy balance for unit cells along the liquid flow direction, from inlet to outlet. The energy balance is solved for each unit cell, and the outlet conditions are calculated. Then, the inlet conditions of the next unit cell are specified based on the outlet conditions of the previous unit cell, and the energy balance is solved for the new unit

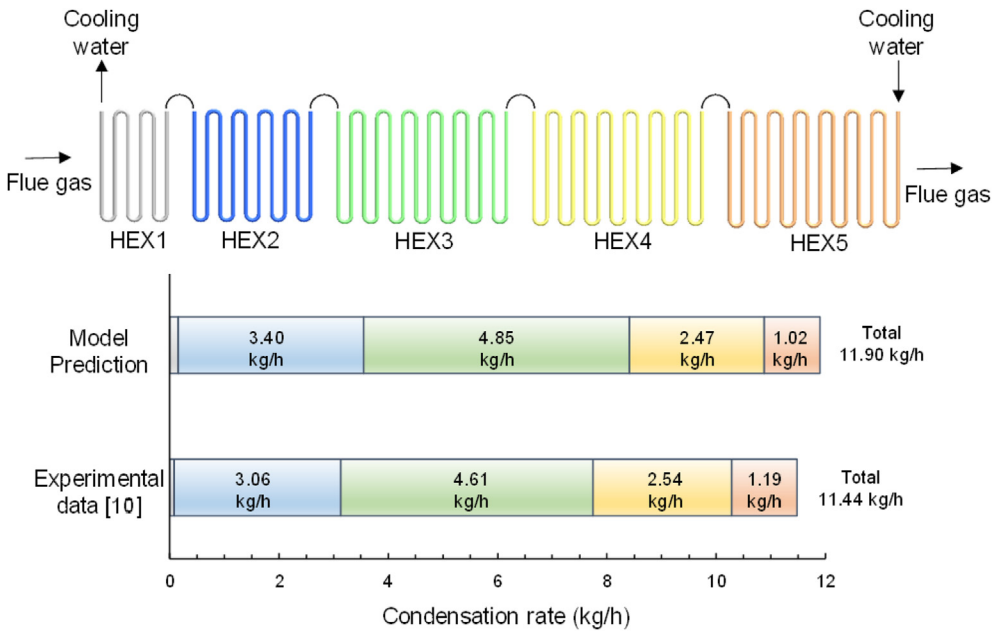

Fig. 4. Comparison of the modeling results and experimental data of Ref. (Jeong et al., 2010).

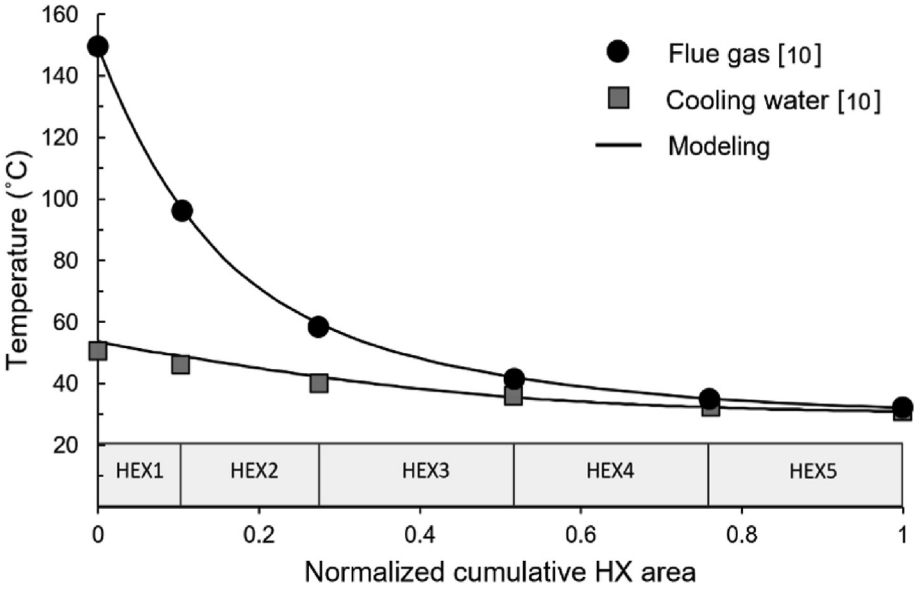

Fig. 5. Comparison of the flue gas and cooling water temperature profiles obtained from our modeling and experimental data from Ref. (Jeong et al., 2010).

cell. This model can predict the performance of both counter and parallel cross-flow condensing heat exchangers. Thus, a code is developed in MATLAB software to solve the governing equations based on the above descriptions using the Newton-Raphson method. The convergence criterion for the Newton-Raphson iteration is chosen as 10^{-6}.

The present model is verified using the experimental data reported by Jeong et al. (2010). They experimentally investigated five heat exchangers' performance connected in series and placed inside a duct through which the flue gas was flowing. All the details regarding the dimension of heat exchangers can be found in Ref. (Jeong et al., 2010). The inlet temperature of cooling water and flue gas were 31 and 149.5 °C, respectively, and the inlet moisture fraction of flue gas was 14.4 vol.% in their study. Moreover, the mass flow rate of cooling water and flue gas were 542.9 and 185.7 kg h^{-1}, respectively. Fig. 4 shows the condensation rates of individual heat exchangers and the total amount of condensation based on our modeling prediction and the experimental results of Ref. (Jeong et al., 2010). Our modeling results agree well with the experimental data. That is, the maximum discrepancy between the experimental data and modeling results for the condensation rates of individual heat exchangers was within 15% and the total condensation rate of heat exchangers was within 5%. Moreover, the modeling results for temperature profiles of the flue gas and cooling water along the five heat exchangers were compared with the experimental data of Ref. (Jeong et al., 2010), and the results are shown in Fig. 5. It should be mentioned that the heat exchangers were in a counter cross-flow arrangement. Therefore, the flue gas entered the heat recovery system through the first heat exchanger, but the cooling water entered the system through the fifth heat exchanger. As shown in Fig. 5, the developed model can accurately describe flue gas and cooling water temperature profiles. Thus, it can be used for characterizing the performance of condensing heat exchangers.

Table 1
Geometric dimensions of heat exchangers under study.

	Diameter (mm)	Thk. (mm)	S_T/d	S_L/d	N_T	N_L	Tube lengths (m)	Total surface area (m^2)
A	8.0	0.7	2	2	19	50	0.3	7.16
B	12.7	0.7	2	2	12	32	0.3	4.60
C	19.0	0.7	2	2	8	21	0.3	3.00
D	25.4	0.7	2	2	6	16	0.3	2.30

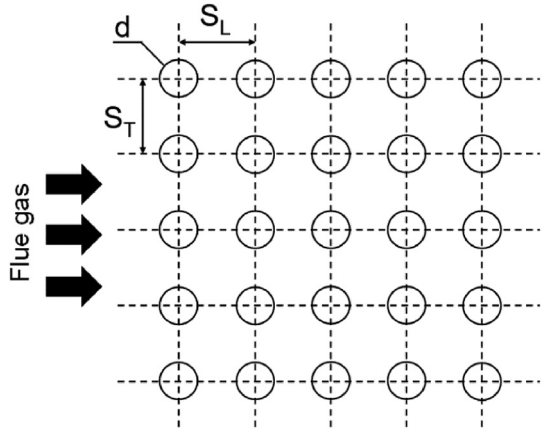

Fig. 6. Schematic of the selected in-line tube arrangement.

3. Results and discussion

In order to investigate the effect of the thermal conductivity of the material on the performance of condensing heat exchangers, four different heat exchangers with various tube sizes are considered with an in-line tube arrangement, which is the most common type of tube-bank heat exchangers in heat recovery systems. The geometric parameters of considered heat exchangers are summarized in Table 1 and illustrated in Fig. 6. It should be mentioned that S_T and S_L are tube pitches in transverse and longitudinal directions, respectively. Moreover, N_T and N_L are the number of tubes arranged in transverse and longitudinal directions, respectively. The frontal area of all the heat exchangers is assumed to be 30 cm × 30 cm, and the length of all the heat exchangers is assumed to be 80 cm, thereby having the same volume and frontal area. Fig. 7 shows the schematic of heat exchangers A and D with 8 and 25.4 mm tube diameters. In addition, the inlet condition of the heat exchangers (A-D) is summarized in Table 2.

Condensation efficiency, the main parameter that controls the performance of a wet heat exchanger, is defined as the mass of condensate over the total mass of water vapor in the inlet flue gas as follows:

$$\eta_{cond} = \dot{m}_{cond}(1+\omega) \Big/ \dot{m}_t \omega \tag{19}$$

Table 2
Inlet condition for heat exchangers A-D.

Inlet temperature of cooling water	25 °C
Inlet temperature of flue gas	100 °C
Mass flow rate of cooling water	1000 kg h^{-1}
Mass flow rate of flue gas	450 kg h^{-1}
Inlet moisture fraction of flue gas	14 vol.%

where, $\dot{m}_t$ is the mass flow rate of flue gas at the inlet of the heat exchanger.

The effect of the thermal conductivity of the material on the condensation efficiency of four condensing heat exchangers is evaluated, and the results are shown in Fig. 8. As expected, increasing the tube thermal conductivity leads to the condensation efficiency enhancement. For all of the heat exchangers with different tube sizes, increasing the thermal conductivity more than a threshold does not significantly affect the condensation performance. However, when the thermal conductivity is less than around 0.75 W $m^{-1}K^{-1}$, the condensation efficiency decreases significantly. For example, the condensation performance of heat exchangers made of fluorine-based plastics with thermal conductivities of less than 0.3 W $m^{-1}K^{-1}$ is significantly less than heat exchangers made of conventional materials for corrosive environments, e.g., stainless steel or titanium with thermal conductivities of 10–15 W $m^{-1}K^{-1}$. However, the results show that using composite polymers with conductive fillers can result in condensation efficiency enhancement of heat and water recovery systems. Furthermore, choosing a heat exchanger with smaller tubes results in a higher condensation efficiency because of a significantly higher surface area than a heat exchanger with larger tubes. However, pressure drop and fouling considerations should be included in the selection of tube sizes.

The effect of tube thermal conductivity on the thermal resistance of the tube's wall is studied. Fig. 9 shows the ratio of the thermal resistance of the tube's wall to the convective thermal resistance of cooling water for different tube sizes and different tube thermal conductivity. It can be seen that, when the thermal conductivity of tubes is less than a threshold (~ 0.75 W.$m^{-1}K^{-1}$), the thermal resistance of the tube's wall (R_{tube}) becomes comparable to the convective heat transfer thermal resistance of the cooling water (R_c); thus, the condensation efficiency decreases significantly. Moreover, due to a smaller surface area, the thermal resistance of the tube's wall is significantly higher for smaller tube diameter and the same wall thickness.

4. Conclusions

Material selection plays a crucial role in the performance of condensing heat exchangers working in a corrosive environment. Materials with impressive corrosion resistance properties and low cost, such as some plastics and polymers, have low thermal properties, which affect the thermal performance of a heat exchanger. In this paper, a new analytical model is developed to investigate the effect of the thermal conductivity of tube material on the condensation efficiency of

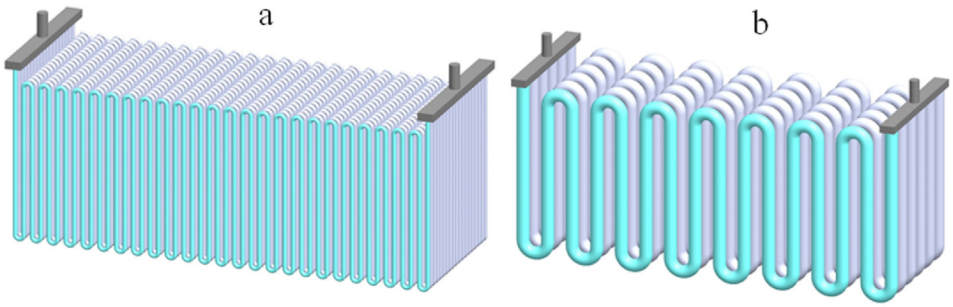

Fig. 7. Schematic of heat exchangers with the same volume and tube diameters of: a) 8 mm; and b) 25.4 mm.

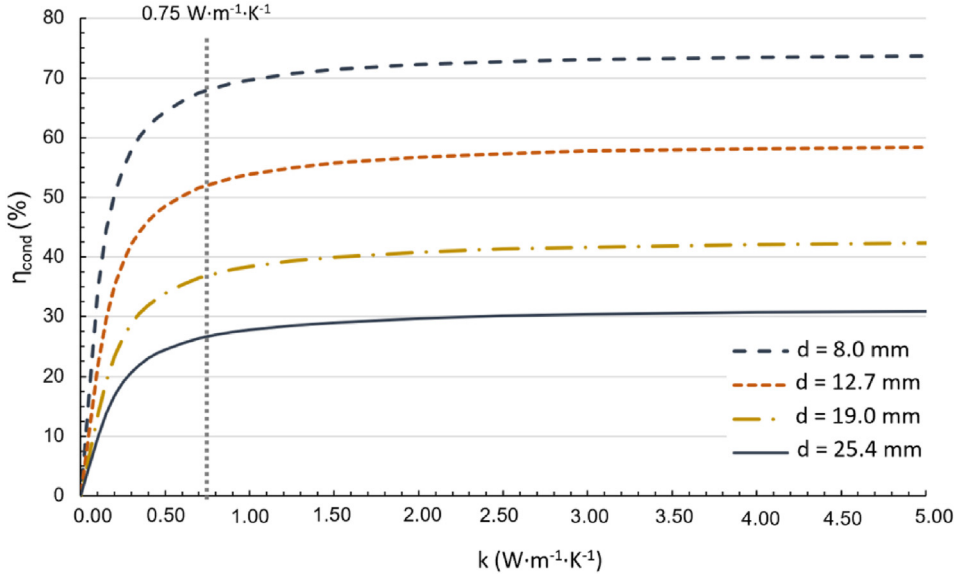

Fig. 8. The effect of the tube thermal conductivity on the condensation efficiency of heat exchangers with different tube sizes.

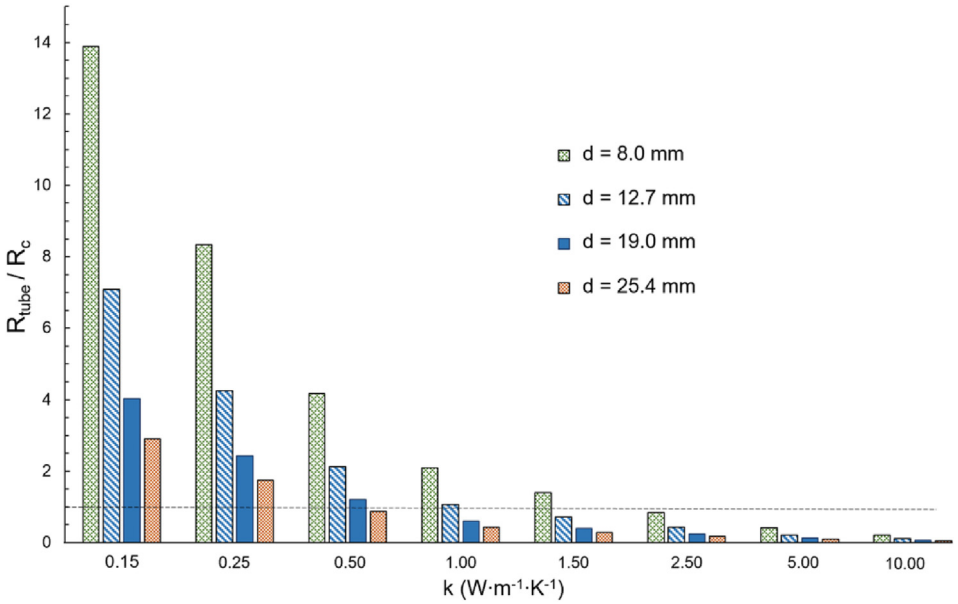

Fig. 9. The ratio of the thermal resistance of tube's wall to the convective thermal resistance of cooling water for different tube sizes and different tube thermal conductivity.

condensing heat exchangers for heat and water recovery from flue gas. The present model can predict the performance of tube-bank heat exchangers in the presence (and absence) of condensation. We observed that increasing thermal conductivity of the tubes to values higher than 0.75 W $m^{-1}K^{-1}$ does not notably further enhance the thermal performance of heat recovery units. However, using materials with thermal conductivity values less than 0.5 W $m^{-1}K^{-1}$ significantly impedes the heat recovery system's efficiency. This finding unlocks the potential of using materials, such as natural graphite, plastics, polymers, and ceramics with thermally-conductive additives for efficient heat and water recovery systems.

Declaration of competing interest

The authors declare that they have no known competing financial interests or personal relationships that could have appeared to influence the work reported in this paper.

Acknowledgement

The authors gratefully acknowledge the financial support of the Natural Sciences and Engineering Research Council of Canada, College-University Idea to Innovation Grant "From Waste to Clean Food" (NSERC CUI2I 501951-16).

References

Ammar, Y., Joyce, S., Norman, R., Wang, Y., Roskilly, A.P., 2012. Low grade thermal energy sources and uses from the process industry in the UK. Appl. Energy 89, 3–20. https://doi.org/10.1016/j.apenergy.2011.06.003.

Bergman, T., Incropera, F., Lavine, A., DeWitt, D., 2011. Fundamentals of Heat and Mass Transfer. John Wiley & Sons, New York. John Wiley & Sons.

Gnielinski, V., 1976. New equations for heat and mass transfer in turbulent pipe and channel flow. Int. Chem. Eng. 16, 359–368.

de Gouw, J.A., Parrish, D.D., Frost, G.J., Trainer, M., 2014. Reduced emissions of CO 2 , NOx, and SO 2 from U.S. power plants owing to switch from coal to natural gas with

combined cycle technology. Earth's Futur 2, 75–82. https://doi.org/10.1002/2013EF000196.
Haddad, C., Périlhon, C., Danlos, A., François, M.-X., Descombes, G., 2014. Some efficient solutions to recover low and medium waste heat: competitiveness of the thermoacoustic technology. Energy Procedia 50, 1056–1069. https://doi.org/10.1016/j.egypro.2014.06.125.
Han, X., Yan, J., Karellas, S., Liu, M., Kakaras, E., Xiao, F., 2017. Water extraction from high moisture lignite by means of efficient integration of waste heat and water recovery technologies with flue gas pre-drying system. Appl. Therm. Eng. 110, 442–456. https://doi.org/10.1016/j.applthermaleng.2016.08.178.
Hwang, K., Song, C. ho, Saito, K., Kawai, S., 2010. Experimental study on titanium heat exchanger used in a gas fired water heater for latent heat recovery. Appl. Therm. Eng. 30, 2730–2737. https://doi.org/10.1016/j.applthermaleng.2010.07.027.
Jeong, K., Kessen, M.J., Bilirgen, H., Levy, E.K., 2010. Analytical modeling of water condensation in condensing heat exchanger. Int. J. Heat Mass Tran. 53, 2361–2368. https://doi.org/10.1016/j.ijheatmasstransfer.2010.02.004.
Jia, L., Peng, X.F., Sun, J.D., Chen, T.B., 2001. An experimental study on vapor condensation of wet flue gas in a plastic heat exchanger. Heat Tran. Res. 30, 571–580. https://doi.org/10.1002/htj.10000.
Levy, E., Bilirgen, H., Jeong, K., Kessen, M., Samuelson, C., Whitcombe, C., 2008. Recovery of Water from Boiler Flue Gas. https://doi.org/10.2172/952467. Pittsburgh, PA, and Morgantown, WV.
Levy, E., Bilirgen, H., DuPoint, J., 2011. Recovery of Water from Boiler Flue Gas Using Condensing Heat Exchangers. https://doi.org/10.2172/1037725. Pittsburgh, PA, and Morgantown, WV (United States).
Li, Y., Yan, M., Zhang, L., Chen, G., Cui, L., Song, Z., Chang, J., Ma, C., 2016. Method of flash evaporation and condensation – heat pump for deep cooling of coal-fired power plant flue gas: latent heat and water recovery. Appl. Energy 172, 107–117. https://doi.org/10.1016/j.apenergy.2016.03.017.
Martins, F., Felgueiras, C., Smitková, M., 2018. Fossil fuel energy consumption in European countries. Energy Procedia 153, 107–111. https://doi.org/10.1016/j.egypro.2018.10.050.
Men, Y., Liu, X., Zhang, T., Xu, X., Jiang, Y., 2019. Novel flue gas waste heat recovery system equipped with enthalpy wheel. Energy Convers. Manag. 196, 649–663. https://doi.org/10.1016/j.enconman.2019.06.026.
Navarro, H.A., Cabezas-Gómez, L., 2005. A new approach for thermal performance calculation of cross-flow heat exchangers. Int. J. Heat Mass Tran. 48, 3880–3888. https://doi.org/10.1016/j.ijheatmasstransfer.2005.03.027.
Ogbonnaya, C., Abeykoon, C., Damo, U.M., Turan, A., 2019. The current and emerging renewable energy technologies for power generation in Nigeria: a review. Therm. Sci. Eng. Prog. 13, 100390. https://doi.org/10.1016/j.tsep.2019.100390.
Shi, X., Che, D., Agnew, B., Gao, J., 2011. An investigation of the performance of compact heat exchanger for latent heat recovery from exhaust flue gases. Int. J. Heat Mass Tran. 54, 606–615. https://doi.org/10.1016/j.ijheatmasstransfer.2010.09.009.
Thomson, G.W., 1946. The antoine equation for vapor-pressure data. Chem. Rev. 38, 1–39. https://doi.org/10.1021/cr60119a001.
Xiong, Y., Niu, Y., Wang, X., Tan, H., 2014. Pilot study on in-depth water saving and heat recovery from tail flue gas in lignite-fired power plant. Energy Procedia 61, 2558–2561. https://doi.org/10.1016/j.egypro.2014.12.045.
Xiong, Y., Tan, H., Wang, Y., Xu, W., Mikulčić, H., Duić, N., 2017. Pilot-scale study on water and latent heat recovery from flue gas using fluorine plastic heat exchangers. J. Clean. Prod. 161, 1416–1422. https://doi.org/10.1016/j.jclepro.2017.06.081.
Zevenhoven, R., Kilpinen, P., 2001. Control of Pollutants in Flue Gases and Fuel Gases. Helsinki University of Technology Espoo, Finland.
Zhang, S., Cheng, X., Shen, F., 2018. Condensation heat transfer with non-condensable gas on a vertical tube. Energy Power Eng. 10, 25–34. https://doi.org/10.4236/epe.2018.104B004.
Žukauskas, A., 1972. Heat transfer from tubes in crossflow. Adv. Heat Tran. 8, 93–160. https://doi.org/10.1016/S0065-2717(08)70038-8.